

Cis,trans,cis or All-cis Geometry in d^0 Octahedral Dioxo Complexes. An IMOMM Study of the Role of Steric Effects

Guada Barea,[†] Agusti Lledos,^{*,†} Feliu Maseras,^{*,‡} and Yves Jean^{*,§}

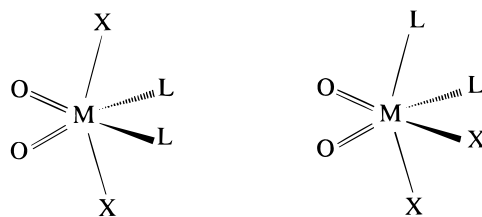
Departament de Química, Universitat Autònoma de Barcelona, 08193 Bellaterra, Catalonia, Spain, Laboratoire de Structure et Dynamique des Systèmes Moléculaires et Solides, UMR 5636, Université de Montpellier II, 34095 Montpellier Cedex 5, France, and Laboratoire de Chimie Théorique, URA 506, Bât. 490, Université de Paris—Sud, 91405 Orsay Cedex, France

Received September 25, 1997

The relative stabilities of two different isomers of d^0 $\text{MoO}_2\text{Cl}_2\text{L}_2$ species are examined for two different complexes with the help of the integrated molecular orbital mechanics method IMOMM. The experimentally reported preference of the $\text{MoO}_2\text{Cl}_2(N,N,N',N'$ -tetramethylethylenediamine) complex for the all-cis arrangement and that of the $\text{MoO}_2\text{Cl}_2(N,N'$ -di-*tert*-butyl-1,4-diaza-1,3-butadiene) complex for the cis,trans,cis arrangement are properly reproduced. The inversion of relative stabilities is shown to be associated to the balance between electronic and steric contributions, the former favoring the cis,trans,cis arrangement and the latter stabilizing the all-cis form.

Several rules are known to govern the geometry and the ligand site occupation in six-coordinate d^0 complexes of $\text{MO}_2\text{X}_2\text{L}_2$ type ($M = \text{Mo}, \text{W}$). These species always present a distorted octahedral geometry,¹ with the oxo ligands cis to each other in order to maximize the back-donation into the empty t_{2g} set orbitals.² Most often, the arrangement of the anionic X and neutral L ligands are trans and cis,³ respectively, with the complexes adopting the *cis*-oxo,*trans*-X,*cis*-L configuration (**1a**; Chart 1). Examples of this configuration include all known complexes with $X = \text{alkyl},^4 \text{OR},^5 \text{SR},^6$ and most complexes with $X = \text{halide}$ (F, Cl, Br).^{7–12} In this latter case, the set of ancillary L ligands may involve either two monodentate ligands (DMF,⁷ $\text{PPh}_3\text{O},^3 \text{H}_2\text{O}^8$) or a single chelating L–L ligand with

Chart 1



1a (*cis*-*trans*-*cis*)

1b (*all*-*cis*)

oxygen^{9–11} or nitrogen¹² atoms bound to the metal. Until recent years, no structure exhibiting the all-cis configuration **1b** had been characterized in this family of compounds.

However, in 1992, the X-ray structure¹³ of $\text{WO}_2\text{Cl}_2(\text{tmen})$ ($\text{tmen} = N,N,N',N'$ -tetramethylethylenediamine) revealed an unusual all-cis configuration. One year later, the molybdenum analogue $\text{MoO}_2\text{Cl}_2(\text{tmen})$ (**2**, Figure 1) was also shown to adopt this all-cis configuration.^{14,15} These unexpected results were rationalized on steric grounds: in the hypothetical *cis*,*trans*,*cis* configuration, steric repulsions would be at work between the four methyl substituents of the tmen ligand and the apical chloro ligands. In the actual all-cis configuration, only two methyl groups develop such unfavorable interactions (Figure 1). An all-cis configuration has also been found (X-ray) for the $\text{MoO}_2\text{-Cl}_2(\text{TMC})$ complex¹⁶ (TMC = tetramethylcyclam). Since the

[†] Universitat Autònoma de Barcelona.

[‡] Université de Montpellier II.

[§] Université de Paris—Sud.

- (1) Brower, D. C.; Templeton, J. L.; Mingos, D. M. P. *J. Am. Chem. Soc.* **1987**, *109*, 5203.
- (2) Mingos, D. M. P. *J. Organomet. Chem.* **1979**, *179*, C29.
- (3) Butcher, R. J.; Penfold, B. R.; Sinn, E. *J. Chem. Soc., Dalton Trans.* **1979**, 668.
- (4) (a) Schrauzer, G. N.; Hughes, L. A.; Strampach, N.; Robinson, P. R.; Schlemper, E. O. *Organometallics* **1982**, *1*, 44. (b) Schrauzer, G. N.; Hughes, L. A.; Strampach, N. *Organometallics* **1983**, *2*, 481. (c) Schrauzer, G. N.; Hughes, L. A.; Schlemper, E. O.; Ross, F.; Ross, D. *Organometallics* **1983**, *2*, 1163. (d) Schrauzer, G. N.; Schlemper, E. O.; Liu, N. H.; Wang, Q.; Rubin, K.; Zhang, X.; Long, X.; Chin, C. S. *Organometallics* **1986**, *5*, 2452. (e) Zhang, C.; Schlemper, E. O.; Schrauzer, G. N. *Organometallics* **1990**, *9*, 1016.
- (5) (a) Chisholm, M. H.; Følting, K.; Huffman, J. C.; Kirkpatrick, C. C. *Inorg. Chem.* **1984**, *23*, 1021. (b) Piarulli, U.; Williams, D. N.; Floriani, C.; Gervasio, G.; Viterbo, D. *J. Chem. Soc., Dalton Trans.* **1995**, 3329.
- (6) Lang, R. F.; Ju, T. D.; Hoff, C. D.; Bryan, J. C.; Kubas, G. J. *J. Am. Chem. Soc.* **1994**, *116*, 9747.
- (7) Florian, L. R.; Corey, E. R. *Inorg. Chem.* **1968**, *7*, 722.
- (8) (a) Taylor, M. J.; Jirong, W.; Rickard, C. E. F. *Polyhedron* **1993**, *12*, 1433. (b) Coddington, J. M.; Taylor, M. J. *J. Chem. Soc., Dalton Trans.* **1990**, 41. (c) Arnaiz, F. J.; Aguado, R.; Sanz-Aparicio, J.; Martínez-Ripoll, M. *Polyhedron* **1994**, *13*, 2745.
- (9) Pierpont, C. G.; Downs, H. H. *Inorg. Chem.* **1977**, *16*, 2970.
- (10) (a) Bowen, S. M.; Duesler, E. N.; McCabe, D. J.; Paine, R. T. *Inorg. Chem.* **1985**, *24*, 1191. (b) Gahagan, M.; Mackie, R. K.; Cole-Hamilton, D. J.; Cupertino, D. C.; Harman, M.; Hurthouse, M. B.; *J. Chem. Soc., Dalton Trans.* **1990**, 2195.

- (11) (a) Kamenar, B.; Penavic, M.; Korpar-Colig, B.; Markovic, B. *Inorg. Chim. Acta* **1982**, *65*, L245. (b) Dreisch, K.; Andersson, C.; Stalhandske, C. *Polyhedron* **1991**, *10*, 2417. (c) Dreisch, K.; Andersson, C.; Hakansson, M.; Jagner, S. *J. Chem. Soc., Dalton Trans.* **1993**, 1045.
- (12) (a) Fenn, R. H. *J. Chem. Soc. A* **1969**, 1764. (b) Sens, I.; Stenger, H.; Müller, U.; Dehnicke, K. *Z. Anorg. Allg. Chem.* **1992**, *610*, 117. (c) Baird, D. M.; Yang, F. L.; Kavanaugh, D. J.; Finness, G.; Dunbar, K. R. *Polyhedron* **1996**, *15*, 2597.
- (13) Dreisch, K.; Andersson, C.; Stalhandske, C. *Polyhedron* **1992**, *11*, 2143.
- (14) Dreisch, K.; Andersson, C.; Stalhandske, C. *Polyhedron* **1993**, *12*, 303.
- (15) Allen, F. H.; Kennard, O. *Chem. Des. Autom. News* **1993**, *8*, 31.

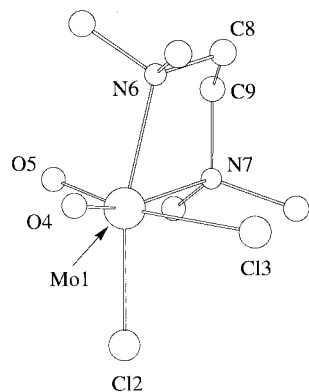


Figure 1. Experimental X-ray structure of the $\text{MoO}_2\text{Cl}_2(\text{tmen})$ complex **2** ($\text{tmen} = N,N,N',N'$ -tetramethylethylenediamine) as taken from the Cambridge Structural Database.^{14,15} Hydrogen atoms are omitted for simplicity.

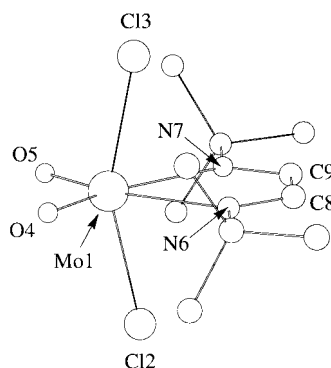


Figure 2. Experimental X-ray structure of the $\text{MoO}_2\text{Cl}_2(\text{Bu}^t\text{-dab})$ complex **3** ($\text{Bu}^t\text{-dab} = N,N'$ -di-*tert*-butyl-1,4-diaza-1,3-butadiene) as taken from the Cambridge Structural Database.^{14,15} Hydrogen atoms are omitted for simplicity.

portion of the macrocycle that coordinates the metal is essentially the tetramethylethylenediamine, as in **2**, the reasons favoring this configuration were believed to be the same. In marked contrast, the $\text{MoO}_2\text{Cl}_2(\text{Bu}^t\text{-dab})$ complex **3** ($\text{Bu}^t\text{-dab} = N,N'$ -di-*tert*-butyl-1,4-diaza-1,3-butadiene) has been shown (X-ray) to exhibit the usual *cis,trans,cis* arrangement, despite the presence of the bulky *tert*-butyl groups on the chelating nitrogen atoms (Figure 2).^{14,15}

The purpose of this work is to study by theoretical means the way the nature of the L ligands can influence the overall structure of $\text{MoO}_2\text{Cl}_2\text{L}_2$ complexes. DFT quantum mechanical calculations were first performed with the unsubstituted monodentate L (NH_3 , **4**) and with the bidentate L–L ethylenediamine (**5**) and 1,4-diaza-1,3-butadiene (**6**) groups as models for the chelating ligands in **3** and **2**, respectively. Both *cis,trans,cis* and all-*cis* configurations were optimized in order to know the “intrinsic” configurational preference for each complex. The *real* complexes **2** and **3** were then studied using the integrated molecular orbital molecular mechanics (IMOMM) computational scheme¹⁷ to check the role of steric factors on the energy difference between *cis,trans,cis* and all-*cis* configurations. IMOMM has already been proved to be well suited for the quantification of steric effects in transition metal complexes with bulky ligands.^{18,19}

Methods of Calculation

Quantum mechanical calculations on the unsubstituted reference complexes **4**, **5**, and **6** were performed with the GAUSSIAN 94 series

of programs.²⁰ Geometry optimizations were carried out using density functional theory (DFT)²¹ with the B3LYP functional.²² A quasirelativistic effective core potential operator was used to represent the 28 innermost electrons of the molybdenum atom.²³ The basis set for the metal atom was that associated with the pseudopotential,²³ with a standard double- ζ LANL2DZ contraction.²⁰ The 6-31G(d) basis set²⁴ was used for the C, N, O, and Cl atoms, and 6-31G for the H atoms.^{24a} To check the accuracy of the energy differences, single-point MP2, MP4(SDTQ),²⁵ and CCSD(T)²⁶ calculations using the B3LYP optimized geometries were also performed on the smallest size complexes ($\text{L} = \text{NH}_3$).

IMOMM calculations on the *real* complexes **2** and **3** were performed with a program built from modified versions of two standard programs: GAUSSIAN92/DFT²⁷ for the quantum mechanics (QM) part and MM3 (92)²⁸ for the molecular mechanics (MM) part. QM calculations were carried out on the unsubstituted complexes **5** and **6** at the B3LYP level, with the basis set described above. MM calculations on the full systems $\text{MoO}_2\text{Cl}_2(\text{tmen})$ (**2**) and $\text{MoO}_2\text{Cl}_2(\text{Bu}^t\text{-dab})$ (**3**) used the MM3 (92) force field.²⁸ The van der Waals parameters for the Mo atom were taken from the UFF force field,²⁹ and torsional contributions involving dihedral angles with the metal atom in terminal position were set to zero. The MM3 (92) default value for the van der Waals radius of chlorine was replaced by 2.47 Å, a value shown previously³⁰ to be more appropriate for inorganic systems. All geometrical parameters were optimized in the calculations except the N–H (1.028 Å) bond distances in the QM part and the N–C (1.434 Å) bond distances in the MM part.

- (18) (a) Ujaque, G.; Maseras, F.; Lledos, A. *Theor. Chem. Acta* **1996**, *94*, 67. (b) Barea, G.; Maseras, F.; Jean, Y.; Lledos, A. *Inorg. Chem.* **1996**, *35*, 6401. (c) Ogasawara, M.; Maseras, F.; Gallego-Planas, N.; Kawamura, K.; Ito, K.; Toyota, K.; Streib, W. E.; Komiya, S.; Eisenstein, O.; Caulton, K. G. *Organometallics* **1997**, *16*, 1979.
- (19) (a) Matsubara, T.; Maseras, F.; Koga, N.; Morokuma, K. *J. Phys. Chem.* **1996**, *100*, 2573. (b) Svensson, M.; Humbel, S.; Morokuma, K. *J. Chem. Phys.* **1996**, *105*, 3654. (c) Matsubara, T.; Sieber, S.; Morokuma, K. *Int. J. Quantum Chem.* **1996**, *60*, 1101. (d) Froese, R. D. J.; Morokuma, K. *Chem. Phys. Lett.* **1996**, *263*, 393. (e) Wakatsuki, Y.; Koga, N.; Werner, H.; Morokuma, K. *J. Am. Chem. Soc.* **1997**, *119*, 360.
- (20) Frisch, M. J.; Trucks, G. W.; Schlegel, H. B.; Gill, P. M. W.; Johnson, B. G.; Robb, M. A.; Cheeseman, J. R.; Keith, T. A.; Petersson, G. A.; Montgomery, J. A.; Raghavachari, K.; Al-Laham, M. A.; Zakrzewski, V. G.; Ortiz, J. V.; Foresman, J. B.; Cioslowski, J.; Stefanov, B. B.; Nanayakkara, A.; Challacombe, M.; Peng, C. Y.; Ayala, P. Y.; Chen, W.; Wong, M. W.; Andres, J. L.; Replogle, E. S.; Gomperts, R.; Martin, R. L.; Fox, D. J.; Binkley, J. S.; Defrees, D. J.; Baker, J.; Stewart, J. J. P.; Head-Gordon, M.; Gonzalez, C.; Pople, J. A. *Gaussian 94*; Gaussian, Inc.: Pittsburgh, PA, 1995.
- (21) (a) Parr, R. G.; Yang, W. *Density Functional Theory of Atoms and Molecules*; Oxford University Press: Oxford, U.K., 1989. (b) Ziegler, T. *Chem. Rev.* **1991**, *91*, 651.
- (22) (a) Lee, C.; Yang, W.; Parr, R. G. *Phys. Rev. B* **1988**, *37*, 785. (b) Becke, A. D. *J. Chem. Phys.* **1993**, *98*, 5648. (c) Stephens, P. J.; Delvin, F. J.; Chabalowski, C. F.; Frisch, M. J. *J. Phys. Chem.* **1994**, *98*, 11623.
- (23) Hay, P. J.; Wadt, W. R. *J. Chem. Phys.* **1985**, *82*, 299.
- (24) (a) Hehre, W. J.; Ditchfield, R.; Pople, J. A. *J. Chem. Phys.* **1972**, *56*, 2257. (b) Hariharan, P. C.; Pople, J. A. *Theor. Chim. Acta* **1973**, *28*, 213. (c) Francl, M. M.; Pietro, W. J.; Hehre, W. J.; Binkley, J. S.; Gordon, M. S.; Defrees, D. J.; Pople, J. A. *J. Chem. Phys.* **1982**, *77*, 3654.
- (25) Møller, C.; Plesset, M. S. *Phys. Rev.* **1934**, *46*, 618.
- (26) (a) Bartlett, R. J. *J. Phys. Chem.* **1989**, *93*, 1697. (b) Bartlett, R. J.; Watts, J. D.; Kucharski, S. A.; Noga, J. *Chem. Phys. Lett.* **1990**, *165*, 513.
- (27) Frisch, M. J.; Trucks, G. W.; Schlegel, H. B.; Gill, P. M. W.; Johnson, B. G.; Wong, M. W.; Foresman, J. B.; Robb, M. A.; Head-Gordon, M.; Replogle, E. S.; Gomperts, R.; Andres, J. L.; Raghavachari, K.; Binkley, J. S.; Gonzalez, C.; Martin, R. L.; Fox, D. J.; Defrees, D. J.; Baker, J.; Stewart, J. J. P.; Pople, J. A. *Gaussian 92/DFT*; Gaussian, Inc.: Pittsburgh, PA, 1993.
- (28) Allinger, N. L. MM3 (92); Quantum Chemistry Program Exchange: Bloomington, IN, 1992.
- (29) Rappé, A. K.; Casewit, C. J.; Colwell, K. S.; Goddard, W. A., III; Skiff, W. M. *J. Am. Chem. Soc.* **1992**, *114*, 10024.
- (30) Ujaque, G.; Maseras, F.; Eisenstein, O. *Theor. Chem. Acc.* **1997**, *96*, 146.

(16) Lachgar, A.; Farrall, P.; Mayer, J. M. *Polyhedron* **1993**, *12*, 2603.

(17) Maseras, F.; Morokuma, K. *J. Comput. Chem.* **1995**, *9*, 1170.

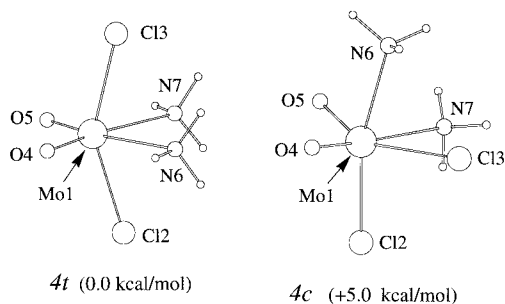


Figure 3. Optimized structures of the cis,trans,cis (**4t**) and all-cis (**4c**) configurations of the $\text{MoO}_2\text{Cl}_2(\text{NH}_3)_2$ model complex at the B3LYP computational level.

$\text{MoO}_2\text{Cl}_2(\text{NH}_3)_2$ Complex. In a first series of calculations, the geometries of both the cis,trans,cis and the all-cis configurations of the $\text{MoO}_2\text{Cl}_2(\text{NH}_3)_2$ complex were fully optimized (B3LYP calculations). In the following, these two isomers are noted **4t** and **4c**, according to the arrangement (trans or cis) of the chloride ligands (Figure 3).

In agreement with the structure of the related experimental complexes involving monodentate ancillary L ligands,^{3,7,8a,c} **4t** was found to be more stable than **4c**. The computed energy difference is 5.0 kcal/mol at the B3LYP level, and single-point energy calculations at the other levels of calculation left this value almost unchanged: 6.1 (MP2), 5.4 (MP4(SDTQ)), and 5.8 kcal/mol (CCSD(T)).

The optimized geometries of the cis,trans,cis isomer (**4t**) exhibit the distorted octahedral arrangement usually found in this family of compounds:^{3,7,8a,c} (i) the $\text{O}=\text{Mo}=\text{O}$ angle value is 106.1° , and the opposite ligand angle ($\text{N6}-\text{Mo}-\text{N7}$) is significantly smaller than 90° (80.1°); (ii) the two axial ligands are bent away from the oxo groups ($\text{Cl2}-\text{Mo}-\text{Cl3} = 150.1^\circ$). Similar angular distortions from the idealized octahedral geometry are found for the less stable all-cis isomer **4c** (104.2 , 75.3 , and 165.1° for the $\text{O}=\text{Mo}=\text{O}$, $\text{Cl3}-\text{Mo}-\text{N7}$, and $\text{Cl2}-\text{Mo}-\text{N6}$ angles, respectively). Comparison between the optimized bond lengths in the two isomers reveals the strong trans effect exerted by the oxo groups: in going from **4t** to **4c**, the $\text{Mo}-\text{Cl3}$ bond length increases by 0.11 \AA while the $\text{Mo}-\text{N6}$ bond length decreases by 0.14 \AA . It is noteworthy that these evolutions found in the reference $\text{MoO}_2\text{Cl}_2(\text{NH}_3)_2$ complex are in excellent agreement with that found in the experimental cis,trans,cis and all-cis molybdenum complexes (**2** and **3**). As a matter of fact, the corresponding $\text{Mo}-\text{Cl}$ and $\text{Mo}-\text{N}$ bond length variations in the experimental structures are $+0.09$ and -0.12 \AA , respectively.¹⁴

Complexes with Unsubstituted Bidentate Ligands. Two complexes were studied, $\text{MoO}_2\text{Cl}_2(\text{HN}=\text{CH}-\text{CH}=\text{NH})$ (**5**) and $\text{MoO}_2\text{Cl}_2(\text{H}_2\text{N}-\text{CH}_2-\text{CH}_2-\text{NH}_2)$ (**6**), in which the 1,4-diaza-1,3-butadiene and the ethylenediamine ligands are the unsubstituted analogues of the bidentate ligands in complexes **3** and **2**, respectively. In both complexes, the cis,trans,cis and the all-cis configurations were optimized, leading to the structures pictured in **5t** and **5c** for the former and **6t** and **6c** for the latter (Figures 4 and 5, respectively).

In the $\text{MoO}_2\text{Cl}_2(\text{HN}=\text{CH}-\text{CH}=\text{NH})$ complex (**5**), **5t** was found to be more stable than **5c** by 7.4 kcal/mol (B3LYP). This result is in agreement with the cis,trans,cis structure reported for the related experimental complex **3**. The geometrical parameters optimized for **5t** are listed in Table 1 (second column) as well as the experimental values for complex **3** (first column). Despite the absence of the bulky tertibutyl groups in our model complex, the agreement between the two sets of values is rather satisfactory. Around the metal center, the mean errors on the bond lengths and the bond angles are 0.035 \AA and 2.3° , respectively. In the bidentate ligand, the bond lengths are almost perfectly reproduced (0.006 \AA (av)) but rather large deviations are found for the angles (4.6° (av)).

Similar calculations were performed on complex **6**. As it was found in the complexes studied above, the cis,trans,cis (**6t**) isomer was found to be more stable than the all-cis (**6c**) isomer, by 4.7 kcal/mol (B3LYP). This value is very close to that found for the model complex **4** with monodentate NH_3 ligands (5.0 kcal/mol), showing that the bidentate

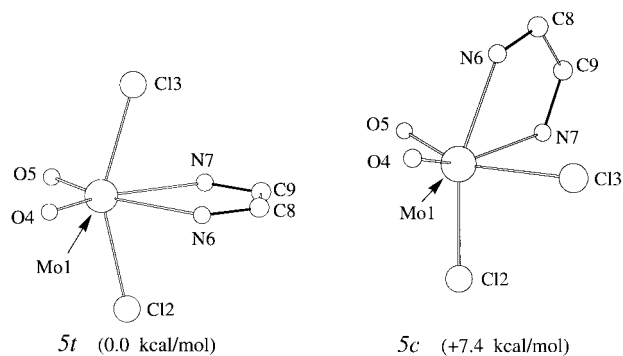


Figure 4. Optimized structures of the cis,trans,cis (**5t**) and all-cis (**5c**) configurations of the $\text{MoO}_2\text{Cl}_2(\text{HN}=\text{CH}-\text{CH}=\text{NH})$ model complex at the B3LYP computational level.

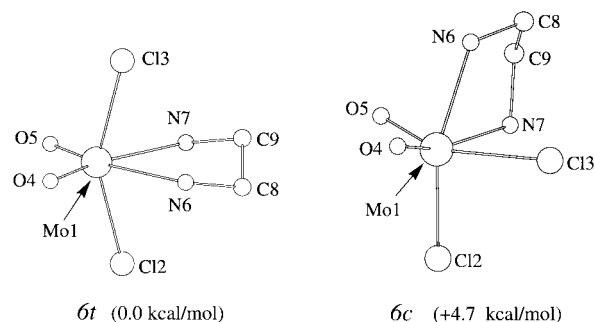


Figure 5. Optimized structures of the cis,trans,cis (**6t**) and all-cis (**6c**) configurations of the $\text{MoO}_2\text{Cl}_2(\text{H}_2\text{N}-\text{CH}_2-\text{CH}_2-\text{NH}_2)$ model complex at the B3LYP computational level.

nature of the ancillary ligand has almost no influence on the energy difference between the two isomers. However, this energetic result is in disagreement with the unusual all-cis structure characterized for the related experimental complex **2**. It is interesting to compare the optimized geometry of the less stable **6c** isomer to that of complex **2** (second and first columns in Table 2, respectively). The bond lengths around the metal center are rather well reproduced (0.037 \AA (av)), that within the bidentate ligand even better (0.014 \AA (av)). The results are, however, less satisfactory for the angles: the mean error is 3.9° around the metal and 4.1° in the bidentate ligand.

It is clear from these results that the optimized geometries of the unsubstituted complexes **5t** and **6c** are in rather good agreement with the structure of the related experimental complexes **3** and **2**, respectively. However, the energy ordering of the cis,trans,cis and the all-cis isomers is correctly reproduced in reference complex **5**, but not in reference complex **6**. A more detailed analysis of the optimized bond angles around the metal center actually shows larger deviations in **6c** than in **5t** (average error 3.9 instead of 2.3°). Furthermore, the reproduction of some bond angles is particularly poor in **6c**: deviations of 8.8 , 8.4 , 6.1 , and 6.1° are found for the $\text{Cl3}-\text{Mo}-\text{O5}$, $\text{Cl3}-\text{Mo}-\text{N6}$, $\text{Cl3}-\text{Mo}-\text{N7}$, and $\text{Cl2}-\text{Mo}-\text{N6}$ angles, respectively, while the largest error in **5t** is only 4.9° . These results constitute the first quantitative indication that substituent effects are larger in **6** than in **5**. The detailed analysis of next section will prove that this is the origin of the different behavior of the complexes.

Geometry Optimizations at the IMOMM Level. Full geometry optimizations of $\text{MoO}_2\text{Cl}_2(\text{Bu}^t\text{-dab})$ (**3**) and $\text{MoO}_2\text{Cl}_2(\text{tmen})$ (**2**) complexes were performed at the IMOMM (B3LYP:MM3) level. The optimized geometries for the cis,trans,cis and the all-cis configurations are pictured in Figure 6 for the former (structures **7t** and **7c**) and in Figure 7 for the latter (structures **8t** and **8c**).

In agreement with the experimental structure of complex **3**, the cis,trans,cis isomer (**7t**) was found to be more stable than the all-cis isomer (**7c**) by 4.7 kcal/mol . This energy difference is slightly lower than that found for the unsubstituted analogue **5** (7.3 kcal/mol), but the energy ordering of the two isomers is preserved upon substitution of the nitrogen centers by the bulky tertibutyl ligands. In marked

Table 1. Selected Geometrical Parameters (Å and deg) for the Experimental Structure of MoO₂Cl₂(Bu^t-dab) (**3**), the B3LYP Optimized Structure of the Cis,trans,cis Isomer of the Model System MoO₂Cl₂(HN=CH-CH=NH) (**5t**), and the IMOMM (B3LYP:MM3) Optimized Structure of the Cis,trans,cis Isomer of MoO₂Cl₂(Bu^t-dab) (**7t**)

	3 (expt) ^a	5t (Becke31yp)	7t (IMOMM)
Mo(1)–Cl(2)	2.356	2.401	2.394
Mo(1)–Cl(3)	2.356	2.401	2.395
Mo(1)–O(4)	1.688	1.704	1.701
Mo(1)–O(5)	1.688	1.704	1.701
Mo(1)–N(6)	2.399	2.439	2.540
Mo(1)–N(7)	2.388	2.438	2.543
N(6)–C(8)	1.267	1.274	1.276
N(7)–C(9)	1.271	1.274	1.276
C(8)–C(9)	1.476	1.484	1.481
Cl(2)–Mo–Cl(3)	156.61	152.1	152.2
Cl(2)–Mo–O(4)	96.9	98.3	98.6
Cl(2)–Mo–O(5)	97.3	98.0	98.3
Cl(2)–Mo–N(6)	80.2	78.5	78.6
Cl(2)–Mo–N(7)	80.7	78.1	78.3
Cl(3)–Mo–O(4)	96.9	98.5	98.5
Cl(3)–Mo–O(5)	97.3	98.1	98.3
Cl(3)–Mo–N(6)	80.2	78.4	78.5
Cl(3)–Mo–N(7)	80.7	78.3	78.4
O(4)–Mo–O(5)	104.5	107.0	104.9
O(4)–Mo–N(6)	93.4	93.6	93.9
O(4)–Mo–N(7)	163.7	159.0	161.2
O(5)–Mo–N(6)	162.0	159.4	161.2
O(5)–Mo–N(7)	91.8	94.0	93.9
N(6)–Mo–N(7)	70.3	65.4	67.3
Mo–N(7)–C(9)	114.4	120.5	114.8
N(7)–C(9)–C(8)	120.2	116.9	121.5
C(9)–C(8)–N(6)	120.4	116.9	121.6
C(8)–N(6)–Mo	114.8	120.4	114.8

^a X-ray data from ref 14.

contrast, an inversion was found for complex **2**, **8c** being more stable than **8t** by 2.4 kcal/mol. This energetic result is now in agreement with the unusual all-cis structure of complex **2**. Since an energy difference of 4.7 kcal/mol in favor of the cis,trans,cis isomer was found in the unsubstituted analogue **6**, it is clear that steric interactions involving methyl groups linked to the nitrogen atoms play a crucial role in the energetic ordering of the two isomers.

Before analyzing in more detail the steric interactions at work in each complex (next section), let us first discuss the geometrical consequences of introducing the substituents (Tables 1 and 2). To do this, we will compare the experimental data (complexes **3** and **2**) with the geometrical parameters optimized for the corresponding isomer in the unsubstituted analogues (B3LYP, **5t** and **6c**) and in the real complexes (IMOMM, **7t** and **8c**). For complex **3**, the average deviation for the angles around the metal center decreases from 2.3 to 1.8°, that for the angles within the bidentate ligand from 4.6 to 0.7°, in going from the unsubstituted reference complex **5t** to the real complex **7t**. Note also that the orientation of the tertibutyl ligands given by the IMOMM calculation in structure **7t** is exactly that found in the experimental structure **3** (Figure 2). For complex **2**, the improvement for the L–M–L angles is even larger, the mean error decreasing from 3.9 to 2.3°. In particular, the values for the angles which came out to be poorly reproduced in the unsubstituted model complex **6c** are substantially improved by the IMOMM optimization of **8c**: the deviations for the Cl3–Mo–O5, Cl3–Mo–N6, Cl3–Mo–N7, and Cl2–Mo–N6 angles decrease from 8.8, 8.4, 6.1, and 6.1° to 5.3, 1.0, 0.4, and 0.3°, respectively (Table 2). On the other hand, the angles within the bidentate ligand are also much more satisfactory, with an average deviation of 1.5 instead of 4.1°. Finally, most of the metal–ligand bond lengths remain almost unchanged upon IMOMM optimizations. A striking exception is, however, found for the Mo–N₆ and Mo–N₇ bonds in both **7t** and **8c** structures. Although these bond lengths were properly reproduced by the B3LYP calculations on the

Table 2. Selected Geometrical Parameters (Å and deg) for the Experimental Structure of MoO₂Cl₂(tmen) (**2**), the B3LYP Optimized Structure of the All-cis Isomer of the Model System MoO₂Cl₂(H₂N–CH₂–CH₂–NH₂) (**6c**), and the IMOMM (B3LYP:MM3) Optimized Structure of the All-cis Isomer of MoO₂Cl₂(tmen) (**8c**)

	2 (expt) ^a	6c (Becke31yp)	8c (IMOMM)
Mo(1)–Cl(2)	2.338	2.329	2.331
Mo(1)–Cl(3)	2.449	2.548	2.478
Mo(1)–O(4)	1.681	1.707	1.700
Mo(1)–O(5)	1.697	1.722	1.721
Mo(1)–N(6)	2.278	2.303	2.416
Mo(1)–N(7)	2.464	2.429	2.676
N(6)–C(8)	1.486	1.488	1.505
N(7)–C(9)	1.478	1.475	1.495
C(8)–C(9)	1.490	1.526	1.536
Cl(2)–Mo–Cl(3)	87.5	91.4	89.3
Cl(2)–Mo–O(4)	104.0	107.6	104.0
Cl(2)–Mo–O(5)	96.9	101.7	98.4
Cl(2)–Mo–N(6)	165.2	159.1	164.9
Cl(2)–Mo–N(7)	89.8	88.0	93.7
Cl(3)–Mo–O(4)	92.7	93.9	96.2
Cl(3)–Mo–O(5)	162.1	153.3	156.8
Cl(3)–Mo–N(6)	84.5	76.1	83.5
Cl(3)–Mo–N(7)	82.1	76.0	81.7
O(4)–Mo–O(5)	103.1	103.9	103.1
O(4)–Mo–N(6)	88.9	90.1	90.0
O(4)–Mo–N(7)	165.1	161.8	162.2
O(5)–Mo–N(6)	87.5	84.0	83.6
O(5)–Mo–N(7)	80.5	81.3	76.0
N(6)–Mo–N(7)	76.7	72.9	72.1
Mo–N(7)–C(9)	103.3	109.4	104.4
N(7)–C(9)–C(8)	111.8	108.6	111.5
C(9)–C(8)–N(6)	111.3	109.9	112.1
C(8)–N(6)–Mo	109.3	115.0	113.1
Cl3–Mo–N6–C8	+69.4	+70.9	+71.6
Mo–N7–C9–C8	+44.0	+46.2	+45.2
N6–Mo–N7–C9	–15.5	–20.9	–17.7

^a X-ray data from ref 14.

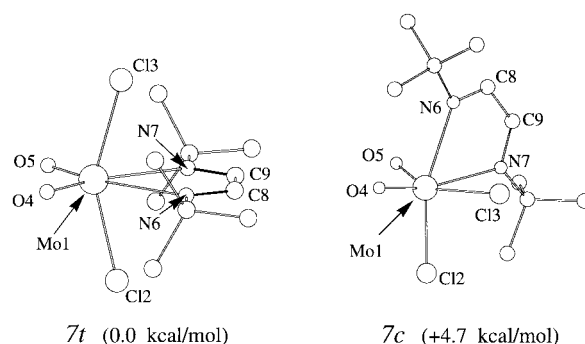


Figure 6. Optimized structures of the MoO₂Cl₂(Bu^t-dab) complex **3** in its cis,trans,cis (**7t**) and all-cis (**7c**) configurations at the IMOMM (B3LYP:MM3) computational level. Hydrogen atoms are omitted for simplicity.

unsubstituted complexes (with errors between 0.025 and 0.050 Å), they are widely overestimated in the substituted complexes, by 0.141 and 0.155 Å in **7t** and by 0.138 and 0.212 Å in **8c** (similar overestimations were found in the less stable isomers **7c** and **8t**). This poor reproduction of the bond lengths is, however, not related to the IMOMM method, because the same result is confirmed by much more expensive calculations at the B3LYP level on the real system.

Quantification of Steric Effects. Although IMOMM is essentially devised as a method for the calculation of accurate geometries and energetics of large systems at a moderate computational cost, it can also be used as a tool for the quantification of steric effects in terms of energy.¹⁸ In this section, we will analyze which of the steric interactions

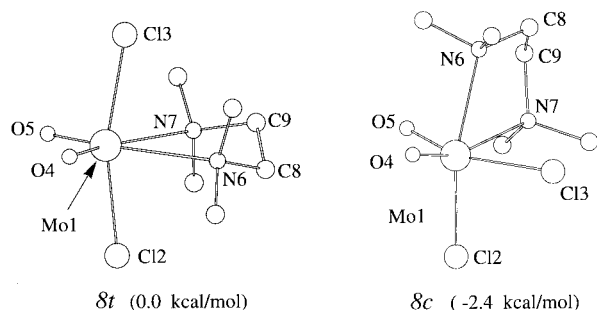


Figure 7. Optimized structures of the $\text{MoO}_2\text{Cl}_2(\text{tmen})$ complex **2** in its cis,trans,cis (**8t**) and all-cis (**8c**) configurations at the IMOMM (B3LYP:MM3) computational level. Hydrogen atoms are omitted for simplicity.

Table 3. Different Contributions (in kcal/mol) to the MM Part of the IMOMM (B3LYP:MM3) Energy of the Two Isomers of $\text{MoO}_2\text{Cl}_2(\text{tmen})$

	8c	8t	$\Delta(\text{trans} - \text{cis})$
compression	0.02	0.03	0.01
bending	1.45	1.78	0.33
bending–bending	–0.14	–0.15	–0.01
stretching–stretching	–0.05	–0.05	0.00
vdW 1,4	8.08	8.52	0.44
vdW other	8.43	12.19	3.76
torsional	2.16	2.45	0.29
torsion–stretching	–0.05	–0.05	0.00
dipole–dipole	0.09	0.10	0.01
total	19.99	24.82	4.83

explain the preference observed in the IMOMM calculation for the unusual structure adopted by **2**.

The IMOMM optimizations of the two isomers of species **8** result in a difference of 2.40 kcal/mol in favor of **8c**. This 2.40 kcal/mol can be decomposed into electronic (quantum mechanics) and steric (molecular mechanics) contributions. It is found that the 2.43 kcal/mol of electronic stabilization of the cis,trans,cis isomer **8t** are compensated by a steric preference of 4.83 kcal/mol for the all-cis isomer **8c**. The steric effects are thus responsible for the stability of **2**. It is interesting to compare this result with that found for complex **7**. In **7**, the steric contribution also favors the all-cis isomer, but only by 2.94 kcal/mol, while the electronic preference for the cis,trans,cis isomer is 7.69 kcal/mol, resulting in a net preference of 4.75 kcal/mol for **7t**.

The molecular mechanics contribution to the total energy can be further divided into its different terms. Table 3 shows this decomposition for the two isomers of **8**, as well as the differences between them. The most significant contribution to the total energy difference of 4.93

Table 4. Contribution (in kcal/mol) to the “VdW other” Term of the Interaction of the Chelating Ligand with Each of the Four Other Ligands in the IMOMM (B3LYP:MM3) Calculation of the Two Isomers of $\text{MoO}_2\text{Cl}_2(\text{tmen})$

	Cl2	Cl3	O4	O5
8c	0.06	3.76	0.24	2.08
8t	4.82	4.82	–0.11	–0.11

kcal/mol comes from the 3.76 kcal/mol of the term labeled as “van der Waals other (vdW other)”, where “vdW other” stands for van der Waals contributions different from 1,4. The MM3 force field places the steric repulsions precisely in this term, so this result is by no means surprising.

Again, the “vdW other” term can be decomposed into its contributions (single interatomic interactions). Table 4 presents the interactions of each of the four other ligands with the bidentate ligand in each of the two isomers of **8**. It is clear that in each complex there are repulsive interactions over 2 kcal/mol with the two ligands perpendicular to the N6–Mo–N7 plane: Cl3 and O5 for **8c**, Cl2 and Cl3 for **8t**. The repulsions with the chloride ligands are always larger than those with the oxo ligands, providing a clear-cut explanation for the steric destabilization of the isomer having both chloride in the sterically hindered sites (**8t**), with respect to the isomer with only one chloride ligand in a sterically hindered site (**8c**).

Conclusions

IMOMM calculations on the real systems do reproduce correctly in both cases the order of stabilities of the cis,trans,cis and all-cis isomers, a result that could not be achieved by pure ab initio calculations on the reference complexes with unsubstituted bidentate ligands. The difference in the nature of the most stable isomer is thus related to steric effects, with the methyl groups of the tmen ligand causing a larger repulsion than the *tert*-butyl groups of Bu^t-dab because of its different orientation in space. It is also shown how the steric preference for the all-cis isomer is associated to the fact that the oxo ligand has a smaller steric bulk than chloride.

Acknowledgment. Y.J. is grateful to the Iberdrola Company for an invitation as Visiting Professor at the Universitat Autònoma de Barcelona. G.B. and A.L. acknowledge financial support from the DGES of Spain (Project No. PB95-0639-CO2-01). The use of computational facilities of the Centre de Supercomputació i Comunicacions de Catalunya (C⁴) are gratefully appreciated as well. Support is also acknowledged from the Accion Integrada Hispano–Francesa (96034/0182).

IC971226E